THE JOURNAL OF BIOLOGICAL CHEMISTRY VOL. 288, NO. 45, pp. 32673–32684, November 8, 2013

Eukaryotic Oligosaccharyltransferase Generates Free Oligosaccharides during *N*-Glycosylation*

Received for publication, June 3, 2013, and in revised form, September 16, 2013 Published, JBC Papers in Press, September 23, 2013, DOI 10.1074/jbc.M113.486985

Yoichiro Harada[‡], Reto Buser[§], Elsy M. Ngwa[§], Hiroto Hirayama[‡], Markus Aebi[§], and Tadashi Suzuki[‡1]

From the [‡]Glycometabolome Team, Systems Glycobiology Research Group, RIKEN-Max Planck Joint Research Center, Global Research Cluster, RIKEN, 2-1 Hirosawa, Wako, Saitama 351-0198, Japan and the [§]Institute of Microbiology, Department of Biology, ETH Zurich, 8093 Zurich, Switzerland

Background: The enzyme generating free oligosaccharides (fOSs) in the lumen of the endoplasmic reticulum (ER) has been unidentified.
Results: Oligosaccharyltransferase (OST), the *N*-glycosylating enzyme, hydrolyzes dolichol-linked oligosaccharides to release the fOSs.
Conclusion: OST is responsible for the generation of fOSs in the ER lumen.
Significance: This study provides a mechanistic insight into the formation of luminal fOSs in yeast.

Asparagine (*N*)-linked glycosylation regulates numerous cellular activities, such as glycoprotein quality control, intracellular trafficking, and cell-cell communications. In eukaryotes, the glycosylation reaction is catalyzed by oligosaccharyltransferase (OST), a multimembrane protein complex that is localized in the endoplasmic reticulum (ER). During *N*-glycosylation in the ER, the protein-unbound form of oligosaccharides (free oligosaccharides; fOSs), which is structurally related to *N*-glycan, is released into the ER lumen. However, the enzyme responsible for this process remains unidentified. Here, we demonstrate that eukaryotic OST generates fOSs. Biochemical and genetic analyses using mutant strains of *Saccharomyces cerevisiae* revealed that the generation of fOSs is tightly correlated with the *N*-glycosylation activity of OST. Furthermore, we present evidence that the purified OST complex can generate fOSs by hydrolyzing dolichol-linked oligosaccharide, the glycan donor substrate for *N*-glycosylation. The heterologous expression of a single subunit of OST from the protozoan *Leishmania major* in *S. cerevisiae* demonstrated that this enzyme functions both in *N*-glycosylation and generation of fOSs. This study provides insight into the mechanism of PNGase-independent formation of fOSs.

N-Glycosylation is a fundamental and evolutionarily conserved post-translational protein modification that occurs in all domains of life (1, 2). In eukaryotes, the glycosylation often occurs co-translationally on nascent polypeptides emerging from the protein-conducting channel in the endoplasmic reticulum (ER)[2] lumen (3, 4). Oligosaccharyltransferase (OST) catalyzes the transfer of the fully assembled glycan, $Glc_3Man_9GlcNAc_2$, from its dolichylpyrophosphate-linked precursor to the target asparagine residue of polypeptide chains.

During the *N*-glycosylation process in mammalian cells, free oligosaccharides (fOSs) are generated in the ER lumen by a yet unclarified mechanism (5, 6), but fOSs are thought to be derived from either *N*-glycosylated proteins or dolichylpyrophosphoryl oligosaccharides (DLOs). The generation of fOSs from glycoproteins suggests that they result from the enzymatic deglycosylation of misfolded glycoproteins destined for proteasomal destruction by a process called ER-associated degradation. This deglycosylation reaction is catalyzed by the cytoplasmic peptide:*N*-glycanase (PNGase; Png1 in *Saccharomyces cerevisiae*) (7, 8), which is highly conserved in eukaryotes.

In *S. cerevisiae*, Png1-mediated cytosolic deglycosylation of glycoproteins is the dominant source for fOSs, as demonstrated by the marked reduction in, but not the complete depletion of, fOSs in *png1*Δ cells (9, 10). The glycoprotein-derived fOSs are catabolized solely by Ams1, a cytosol-vacuolar α-mannosidase (9, 10). On the other hand, the molecular basis underlying the Png1-independent generation of fOSs in *S. cerevisiae* remains to be explored.

EXPERIMENTAL PROCEDURES

Yeast Strains—Yeast strains used in this study were listed in Table 1. Various deletion mutants were generated by the PCR-based gene deletion technique (11, 12).

Plasmids—Plasmids used in this study are listed in Table 2. pOST3 and pOST6 were generated using the In-Fusion HD cloning kit (Takara), genomic DNA from BY4741 as a template, and the primers listed in Table 3. Briefly, open reading frame of Ost3 and Ost6 that is flanked by 500 bp upstream of the initiation codon and 200 bp downstream of the stop codon was amplified, using the yeast genomic DNA (100 ng) and primers listed in Table 3, by KOD-Plus DNA polymerase (Toyobo) according to the manufacturer's instructions. YEp352 vector

* This study was partly supported by Grants-in-aid for Scientific Research 24770134 (to Y. H.) and 25291030 (to T. S.) from the Ministry of Education, Culture, Sports, Science and Technology of Japan; the Global Center of Excellence Program (to T. S.); and Swiss National Science Foundation Grant 31003A_127098 (to M. A.).
[1] To whom correspondence should be addressed. Tel.: 81-48-467-9628; Fax: 81-48-467-9626; E-mail: tsuzuki_gm@riken.jp.
[2] The abbreviations used are: ER, endoplasmic reticulum; PNGase, peptide:*N*-glycanase; PA-, pyridylaminated; OST, oligosaccharyltransferase; fOS, free oligosaccharide; DLO, dolichylpyrophosphoryl oligosaccharide; SD, selective dropout; CPY, carboxypeptidase Y; G3M9, $Glc_3Man_9GlcNAc_2$.

TABLE 1
Yeast strains used in this study

Name	Genotypes	Sources
*ams1*Δ	*MAT***a** *his3*Δ*1 leu2*Δ*0 met15*Δ*0 ura3*Δ*0 ams1*Δ*::kanMX4* BY4741	Open Biosystems
*png1*Δ	*MAT***a** *his3*Δ*1 leu2*Δ*0 met15*Δ*0 ura3*Δ*0 png1*Δ*::kanMX4* BY4741	Open Biosystems
*png1*Δ *ams1*Δ	*MAT***a** *his3*Δ*1 leu2*Δ*0 met15*Δ*0 ura3*Δ*0 ams1*Δ*::kanMX4 png1*Δ*::His3MX6* BY4741	This study
*png1*Δ *ams1*Δ *ost3*Δ	*MAT***a** *his3*Δ*1 leu2*Δ*0 met15*Δ*0 ura3*Δ*0 ams1*Δ*::kanMX4 png1*Δ*::His3MX6 ost3*Δ*::hphNT1* BY4741	This study
*png1*Δ *ams1*Δ *ost5*Δ	*MAT***a** *his3*Δ*1 leu2*Δ*0 met15*Δ*0 ura3*Δ*0 ams1*Δ*::kanMX4 png1*Δ*::His3MX6 ost5*Δ*::hphNT1* BY4741	This study
*png1*Δ *ams1*Δ *ost6*Δ	*MAT***a** *his3*Δ*1 leu2*Δ*0 met15*Δ*0 ura3*Δ*0 ams1*Δ*::kanMX4 png1*Δ*::His3MX6 ost6*Δ*::hphNT1* BY4741	This study
*png1*Δ *ams1*Δ *ost3*Δ *ost6*Δ	*MAT***a** *his3*Δ*1 leu2*Δ*0 met15*Δ*0 ura3*Δ*0 ams1*Δ*::kanMX4 png1*Δ*::His3MX6 ost3*Δ*::hphNT1 ost6*Δ*::natNT2* BY4741	This study
*png1*Δ *ams1*Δ *alg6*Δ	*MAT***a** *his3*Δ*1 leu2*Δ*0 met15*Δ*0 ura3*Δ*0 ams1*Δ*::kanMX4 png1*Δ*::His3MX6 alg6*Δ*::hphNT1* BY4741	This study
*png1*Δ *atg19*Δ	*MAT***a** *his3*Δ*1 leu2*Δ*0 met15*Δ*0 ura3*Δ*0 png1*Δ*::kanMX4 atg19*Δ*::hphNT1* BY4741	This study
*png1*Δ *ams1*Δ *gls1*Δ *mns1*Δ *htm1*Δ	*MAT***a** *his3*Δ*1 leu2*Δ*0 met15*Δ*0 ura3*Δ*0 ams1*Δ*::His3MX6 png1*Δ*::hphNT1 gls1*Δ*::LEU2 mns1*Δ*::natNT2 htm1*Δ*::kanMX4* BY4741	This study
OST4-FLAG	*MAT* ***a*** *leu2-3,112 trp1-1 can1-100 ura3-1 ade2-1 his3-11,15 OST4–3×FLAG::HisMX6*	This study

TABLE 2
Plasmids used in this study

Name	Plasmids	Source/Reference
pOST3	YEp352-*OST3*	This study
pOST6	YEp352-*OST6*	This study
pLmSTT3D (WT)	pRS425-GPD-*LmSTT3D* (WT)	Ref. 36
pLmSTT3D (E102A)	pRS425-GPD-*LmSTT3D* (E102A)	This study
pLmSTT3D (D104A)	pRS425-GPD-*LmSTT3D* (D104A)	This study
pLmSTT3D (D223N)	pRS425-GPD-*LmSTT3D* (D223N)	This study
pLmSTT3D (E225Q)	pRS425-GPD-*LmSTT3D* (E225Q)	This study
pLmSTT3D (D223N E225Q)	pRS425-GPD-*LmSTT3D* (D223N E225Q)	This study
pLmSTT3D (D639A)	pRS425-GPD-*LmSTT3D* (D639A)	This study
pLmSTT3D (D698A)	pRS425-GPD-*LmSTT3D* (D698A)	This study
pLmSTT3D (K701A)	pRS425-GPD-*LmSTT3D* (K701A)	This study
pScSTT3	pRS425-GPD-*ScSTT3*	This study

was amplified using the primers listed in Table 3 by PrimeSTAR Max DNA polymerase (Takara) according to the manufacturer's instructions. The PCR product of YEp352 vector was digested with DpnI (0.5 μl, 10 units; Toyobo) for 1 h at 37 °C and terminated by heating for 15 min at 75 °C. All of the PCRs were purified with the NucleoSpin Gel and PCR Clean-Up kit (Clontech) and subjected to recombination with the In-Fusion HD cloning kit. The reaction products were used for transformation of *Escherichia coli* DH5α strain (Toyobo). pScSTT3 was generated with In-Fusion HD cloning kit as described above, except that their coding sequences were amplified by using primers listed in Table 3. pRS425-GPD vector was amplified, using the primers listed in Table 3, by PrimeSTAR Max DNA polymerase.

Mutagenesis—Mutagenesis of the pLmSTT3D plasmid was carried out using PrimeSTAR Max DNA polymerase (Takara) and the primers listed in Table 3.

Cell Culture—The standard yeast medium was used. The medium and 20% (w/v) glucose were separately autoclaved, and the autoclaved glucose was added to the medium at a concentration of 2% just before use. The yeast cells were spread from the 15% (v/v) glycerol stock onto YPD plates and grown for 3 days at 30 °C. The fresh single colony was inoculated in 50 ml of synthetic complete medium or selective dropout (SD) medium lacking appropriate nutrients and incubated for 24 h at 30 °C. For transformants, a fresh colony was first inoculated in 5 ml of the SD medium lacking appropriate nutrients for 24 h at 30 °C. The preculture was diluted to 0.2 A_{600} unit in 50 ml of the same medium and grown for 24 h at 30 °C.

Preparation of fOSs—The yeast cells were harvested and washed twice with 10 ml of the ice-cold phosphate-buffered saline (PBS). The washed cells were resuspended in 1 ml of lysis buffer (20 mM Tri-HCl, pH 7.4, and 10 mM EDTA), and then 3 ml of the ice-cold ethanol were added. The cells were homogenized by three 10-s vigorous agitations separated by 5-min cooling periods on ice. The homogenate was centrifuged at 15,000 × *g* for 15 min, and the supernatant was recovered as the soluble oligosaccharide fraction and evaporated to dryness. The dried soluble oligosaccharide fraction was desalted on the column containing a stack of AG50-X8 (250 μl, 200–400 mesh, H^+ form) and AG1-X2 (250 μl, 200–400 mesh, acetate form) (Bio-Rad), followed by an InertSep GC column (150 mg/3 ml) (GL Sciences).

Subcellular Fractionation—The yeast cells were grown in YPD medium for 24 h to reach the cell density at ~10 A_{600} units, resuspended in 10 ml of TSD buffer (100 mM Tris sulfate, pH 9.4, and 10 mM DTT), and incubated for 10 min at room temperature. The cells were harvested and resuspended in 5 ml of spheroplasting buffer (0.75× YP, 2% glucose, 1.2 M sorbitol, and 20 mM Tris-HCl, pH 7.4) supplemented with 0.5 mg of zymolyase 100T (Seikagaku Co.). After incubation for 30 min at 30 °C with gentle agitations, the cells were harvested and gently washed twice with 10 ml of the ice-cold PBS containing 1.2 M sorbitol. The cells were resuspended in 300 μl of B88 (20 mM Hepes-KOH, pH 7.4, 300 mM KCl, 5 mM $MgCl_2$, and 200 mM sorbitol) and homogenized in a Potter-Elvehjem homogenizer by 20 strokes on ice. The homogenate was centrifuged at 1,000 × *g* for 5 min at 4 °C, and the supernatant (S1) was recovered. These homogenization and centrifugation steps were

TABLE 3
Primers used in this study

Primers	5′ → 3′	Notes
E102A-F	gatacctgatccacgcgttcgacccgtggtt	Mutagenesis
E102A-R	aaccacgggtcgaacgcgtggatcaggtatc	Mutagenesis
D104A-F	ctgatccacgagttcgccccgtggttcaactac	Mutagenesis
D104A-R	gtagttgaaccacggggcgaactcgtggatcag	Mutagenesis
D223N-F	atggcgggtgagttcaacaacgagtgcatcg	Mutagenesis
D223N-R	cgatgcactcgttgttgaactcacccgccat	Mutagenesis
E225Q-F	gtgagttcgacaaccagtgcatcgccgtc	Mutagenesis
E225Q-R	gacggcgatgcactggttgtcgaactcac	Mutagenesis
D639A-F	ttggcctggtgggcctacggctaccag	Mutagenesis
D639A-R	ctggtagccgtaggcccaccaggccaa	Mutagenesis
D698A-F	gggcagagcggcgccctgatgaagtca	Mutagenesis
D698A-R	tgacttcatcagggcgccgctctgccc	Mutagenesis
K701A-F	gcggcgacctgatggcgtcaccgcacatgg	Mutagenesis
K701A-R	ccatgtgcggtgacgccatcaggtcgccgc	Mutagenesis
Ost3-Inf-F	gaattcgagctcggtacccggggatccgatgtcattcccggcggctc	Cloning
Ost3-Inf-R	aagcttgcatgcctgcaggtcgactggactaggcagcctcacaaa	Cloning
Ost6-Inf-F	gaattcgagctcggtacccggggatcctgtctgagttaggagccaac	Cloning
Ost6-Inf-R	aagcttgcatgcctgcaggtcgacttcattcctgtgtgatttaa	Cloning
YEp352-Inf-F	gtcgacctgcaggcatgc	Cloning
YEp352-Inf-R	ggatccccgggtaccgag	Cloning
ScSTT3-Inf-F	gggctgcaggaattcatgggatccgaccggtcg	Cloning
ScSTT3-Inf-R	ggtatcgataagcttttagactctcaagcctaa	Cloning
p425GPD-Inf-F	aagcttatcgataccgtc	Cloning
p425GPD-Inf-R	gaattcctgcagcccggg	Cloning

repeated once on the pellet fraction under the same conditions as described above. The combined S1 fraction was centrifuged at 15,000 × *g* for 5 min at 4 °C, and the supernatant (S15) was recovered. The pellet (P15) was washed once with 300 μl of B88. The S15 fraction was ultracentrifuged at 100,000 × *g* for 20 min at 4 °C, and the supernatant (S100) was recovered as the cytosol fraction. The P15 and P100 were resuspended in 600 μl of B88. To prepare the soluble oligosaccharide fraction, ice-cold ethanol was added to a final concentration of 75% and incubated for 15 min at 0 °C. After centrifugation at 15,000 × *g* for 15 min, the supernatant was evaporated to dryness.

Preparation of DLOs—The yeast cells were cultured, harvested, and washed as described above and resuspended in 2 ml of methanol. After the addition of an equal volume of glass beads (0.5 mm, Yasui Kikai, Kyoto, Japan), the cells were homogenized with a bead beater (Yasui Kikai) by three 1-min vigorous agitations separated by 1-min cooling periods on ice. The homogenate was centrifuged at 3,000 × *g* for 5 min, and the pellet was further washed twice with 5 ml of methanol. The washed pellet was extracted twice with 5 ml of chloroform/methanol (2:1 by volume). The pellet was dried under a nitrogen stream and extracted twice with 5 ml of methanol/water (1:1 by volume) supplemented with 4 mM $MgCl_2$. The DLOs were extracted twice from the pellet by incubation with 5 ml of chloroform/methanol/water (10:10:3 by volume) for 10 min at 37 °C. The supernatant was evaporated to dryness. The residual pellet was re-extracted twice with 1 ml of chloroform/methanol/water (10:10:3 by volume). The resultant supernatant was evaporated to dryness. The pellet was incubated with 1 ml of 20 mM HCl in isopropyl alcohol/water (1:1 by volume) for 30 min at 100 °C. After it was evaporated to dryness, the pellet was extracted three times with 1 ml of water and desalted on an InertSep GC column and then on the AG50-X8 and AG1-X2 column.

Preparation of N-Glycans—The yeast cells were cultured, harvested, and washed twice with 15 ml of water. The cell pellet was resuspended in 1 ml of 10 mM sodium citrate buffer, pH 6.0, and autoclaved for 2 h at 121 °C. After centrifugation at 15,000 × *g* for 5 min, the supernatant was incubated with 3 ml of ethanol for 15 min on ice. After centrifugation at 15,000 × *g* for 15 min, the pellet was dried and dissolved in 200 μl of 0.1 M ammonium bicarbonate with 1 mg/ml trypsin. After incubation for 1 h at 37 °C, trypsin was inactivated by heating for 10 min at 100 °C, and PNGase F (5 units; Roche Applied Science) was added. The reaction mixture was further incubated for 16 h at 37 °C. After inactivation by heating for 5 min at 100 °C, the specimen was desalted on the AG50-X8 and AG1-X2 column and then on an InertSep GC column.

Pyridylamination—Fluorescent labeling of the soluble oligosaccharides with 2-aminopyridine was carried out as described previously (10, 13). Briefly, the dried sample was incubated in 20 μl of 2.76 g/ml 2-aminopyridine in acetate for 1 h at 80 °C. After the reaction, 20 μl of 500 mg/ml dimethylamine boran in acetate was added to the mixture and further incubated for 1 h at 80 °C. Excess amounts of 2-aminopyridine was removed by a MonoFas silica gel spin column (GL Sciences) according to the manufacturer's instructions.

Preparation of the Pyridylaminated Standard Glycans—The pyridylaminated $Man_1GlcNAc_2$ (PA-$Man_1GlcNAc_2$) was prepared from *N*-glycans released from bovine ribonuclease B (Sigma) by PNGase F (Roche Applied Science), which were further digested with jack bean α-mannosidase (Seikagaku Co.) as described under "Glycosidase Digestions."

Size Fractionation HPLC—PA-glycans were separated by size fractionation HPLC with a Shodex NH2P-50 4E column (4.6 × 250 mm; Shodex), as reported previously (10). The elution was achieved by two solvent gradients: solvent A (93% acetonitrile in 0.3% acetate (pH adjusted to 7.0 with ammonia)) and solvent B (20% acetonitrile in 0.3% acetate (pH adjusted to 7.0 with ammonia)). The flow rate was 0.8 ml/min. The column temperature was 25 °C. The gradient program was as follows: 0–5 min, isocratic 3% solvent B; 5–8 min, 3–33% solvent B; 8–40 min, 33–71% solvent B; 40–60 min, isocratic 3% solvent B. Fluores-

TABLE 4
Quantitation of the PA-labeled fOSs from *png1*Δ *ams1*Δ cells

Glycan ID[a]	Amounts[b]		Number of hexoses shifted after jack bean α-mannosidase digestion[c]	Number of hexoses shifted after α1,2-mannosidase digestion[d]	Number of hexoses shifted after α1,2-mannosidase and α1,6-mannosidase double digestion[e]	Glucose unit[g]
	*png1*Δ *ams1*Δ	*ams1*Δ				
	pmol/100 A_{600}					
a	2.0	134.8	6	2	ND[f]	5.76
b-1	9.1	167.4	7	3	ND	4.91
b-2	1.1	45.1	7	2	3	5.75
c	1.6	28.6	8	3	4	4.86
Total amounts	13.8	375.9				

[a] Glycan ID was based on Fig. 1*B*.
[b] Amounts of the fOSs were estimated from peak area of PA-Glc_6 in dual-gradient, reversed-phase HPLC (14).
[c] PA-fOSs were isolated in dual-gradient, reversed-phase HPLC (14) and digested with jack bean α-mannosidase. The digests were analyzed by size fractionation HPLC.
[d] PA-fOSs were isolated in dual-gradient, reversed-phase HPLC (14) and digested with α1,2-mannosidase. The digests were analyzed by size fractionation HPLC.
[e] PA-fOSs were isolated in dual-gradient, reversed-phase HPLC (14) and double digested with α1,2-mannosidase and α1,6-mannosidase. The digests were analyzed by size fractionation HPLC.
[f] ND, not done.
[g] Glucose units of the fOSs were determined by dual-gradient, reversed-phase HPLC (14).

cence of the labeled glycans was detected at the excitation wavelength (310 nm) and the emission wavelength (380 nm).

For Figs. 2*E*, 3 (*B* and *D*), 4 (*B* and *C*), 5 (*A*, *B*, and *F*), and 6 (*A*–*C*) and Table 5, the amounts of PA-oligosaccharides were estimated by size fractionation HPLC, based on the peak area of PA-glucose hexamer (PA-Glc_6) included in the PA-glucose oligomer (degree of polymerization = 3–15; Takara). To determine the sizes of the fOSs generated in *png1*Δ *atg19*Δ cells (Table 5), the isolated peaks in the size fractionation HPLC were digested with jack bean α-mannosidase, as described under "Glycosidase Digestions." The digests were reanalyzed by size fractionation HPLC under the same conditions. As a control, the standard $Man_1GlcNAc_2$, the expected product generated by jack bean α-mannosidase, was also analyzed in parallel to make sure that the fOSs are structurally related to the *N*-glycans.

Dual-gradient, Reversed-phase HPLC—Glycan isomers were separated by dual-gradient, reversed-phase HPLC with an Inertsil ODS-3 column (2.1-mm inner diameter × 150 mm; GL Sciences) (14). Elution was achieved by two solvent gradients: solvent A (0.1 M ammonium acetate buffer, pH 6.4) and solvent B (0.1 M ammonium acetate buffer, pH 4.0, and 0.5% 1-butanol). The flow rate was 200 μl/min. The column temperature was 25 °C. The gradient program was as follows: 0–10 min, isocratic 99% solvent A; 10–110 min, 99–30% solvent A; 110–150 min, isocratic 99% solvent A. Fluorescence of the labeled glycans was detected at the excitation wavelength (320 nm) and the emission wavelength (400 nm). Glucose units and amounts of each PA-fOS were determined as described previously (14). For Table 4 and Fig. 2 (*C* and *D*), fOSs and DLOs were quantitated by dual-gradient, reversed-phase HPLC.

To unambiguously determine the structure of $Man_1GlcNAc_2$ in Table 5, the isolated corresponding peaks in the size fractionation HPLC were analyzed by the dual-gradient, reversed-phase HPLC in parallel with the standard PA-$Man_1GlcNAc_2$. The structural identity was judged by their identical elution position.

Glycosidase Digestions—The PA-glycans were incubated with 5 milliunits of endoglycosidase H (Roche Applied Science) in 20 μl of 10 mM sodium acetate buffer, pH 5.5, for 16 h at 37 °C. The numbers of mannose residues of the labeled glycans were determined by exoglycosidase digestions with the Jack bean α-mannosidase (40 milliunits; Seikagaku Co.) in 20 μl of 10 mM sodium citrate buffer, pH 4.5, or *Aspergillus saitoi* α1,2-mannosidase (0.5 milliunit; Seikagaku Co.) in 20 μl of 10 mM sodium acetate buffer, pH 5.5, for 16 h at 37 °C. For the enzyme digestion with *Xanthomonas manihotis* α1,6-mannosidase (New England Biolabs), the PA-glycans were incubated with 40 units of *X. manihotis* α1,6-mannosidase together with 40 milliunits of *A. saitoi* α1,2-mannosidase in 20 μl of 50 mM sodium citrate buffer, pH 4.5, supplemented with 0.1 mg/ml bovine serum albumin for 16 h at 37 °C. The reaction was terminated by the addition of 80 μl of water, followed by the addition of 300 μl of ethanol. After centrifugation at 15,000 × *g* for 15 min, the supernatant was evaporated to dryness and dissolved in a small volume of water.

TABLE 5
Quantitation of the PA-fOSs from *png1*Δ *ams1*Δ, *png1*Δ, and *png1*Δ *atg19*Δ cells

Glycan structures	Amounts (relative amounts)[a]		
	*png1*Δ *ams1*Δ	*png1*Δ	*png1*Δ *atg19*Δ
	pmol/25 A_{600} (%)		
$Man_1GlcNAc_2$	ND[b]	0.4 (3.9)	39.4 (46.1)
$Man_2GlcNAc_2$	ND[b]	1.4 (15.5)	23.2 (27.2)
$Man_3GlcNAc_2$	ND[b]	0.5 (5.9)	6.9 (8.0)
$Man_4GlcNAc_2$	ND[b]	0.4 (4.1)	2.1 (2.5)
$Man_5GlcNAc_2$	ND[b]	1.1 (11.5)	2.2 (2.5)
$Man_6GlcNAc_2$	ND[b]	1.0 (10.5)	4.0 (4.7)
$Man_7GlcNAc_2$	1.1 (16.5)	1.3 (14.2)	4.4 (5.2)
$Man_8GlcNAc_2$	5.0 (75.3)	2.9 (31.7)	3.1 (3.7)
$Man_9GlcNAc_2$	0.5 (8.2)	0.2 (2.7)	0.1 (0.1)
Total amount	6.6 (100)	9.2 (100)	85.4 (100)

[a] The amounts of fOSs were estimated from peak area of PA-Glc_6 in size fractionation HPLC.
[b] ND, not detected.

Western Blot—Yeast cells (10 A_{600} units) were harvested and incubated in 200 μl of 0.1 M NaOH for 5 min at room temperature. After harvesting the cells, the pellet was resuspended in 100 μl of water, and then 100 μl of 2× SDS sample buffer (125 mM Tris-HCl, pH 6.8, 4% SDS, 20% glycerol, 0.01% bromphenol blue, and 10% β-mercaptoethanol) were added. The cell suspension was heated for 5 min at 100 °C. After a centrifugation at 15,000 × *g* for 5 min, the supernatant (equivalent to 0.5 A_{600} unit) was separated by SDS-PAGE and analyzed by Western blot with anti-carboxypeptidase Y (CPY) (10A5, Invitrogen), anti-Kar2 (y-115, Santa Cruz Biotechnology, Inc.), and anti-3-phosphoglycerate kinase (22C5, Invitrogen) antibodies. Visualization was performed with a LAS-3000 mini (Fujifilm).

For the detection of LmStt3D-HA, the yeast cells (500 A_{600} units) were resuspended in 1 ml of PBS, and an equal volume of the glass beads (0.5 mm) was added. The cells were lysed by three 1-min periods of bead beating separated by 1-min cooling period. The lysate was centrifuged at 1,000 × *g* for 5 min, and the supernatant was further centrifuged at 6,000 × *g* for 5 min. The supernatant was ultracentrifuged at 100,000 × *g* for 20 min. The pellet (microsomes) was resuspended in 100 μl each of a lysis buffer (20 mM Tris-HCl, pH 7.4, and 10 mM EDTA) and 2× SDS sample buffer. To denature, the sample was incubated for 1 h at 37 °C. 20 μl of the sample were analyzed by SDS-PAGE, followed by Western blot with anti-HA (F-7, Santa Cruz Biotechnology, Inc.) and anti-dolichol phosphate mannose synthase 1 (DPM1) (5C5, Invitrogen) antibodies.

*Plasmid Shuffling Assay—stt3*Δ cells (*MATa met15 lys2 stt3*Δ::*KanMX4*) that have been complemented with YEp352-GPD-LmSTT3D-HA were transformed with pLmSTT3Ds or p425GPD empty vector and selected on the SD plate lacking leucine and uracil for 2 days at 30 °C. The transformants were grown in SD medium lacking leucine and uracil for 2 days at 30 °C. The cells (15 A_{600} units) were serially diluted 5-fold in water, and 5 μl of the cell suspension were spotted on the SD plate lacking leucine and uracil and one lacking leucine supplemented with 1 mg/ml 5-fluoroortic acid. The cells were grown for 6 days at 23 °C.

Purification of the OST Complex Containing Ost4-FLAG—The yeast OST complex containing Ost4-FLAG was purified as described previously (15) with slight modifications. The microsomes (16,000 eq) (44) that were prepared from yeast strain W303-1A expressing Ost4-FLAG (*MAT**a** leu2-3,112 trp1-1 can1-100 ura3-1 ade2-1 his3-11,15 OST4-3×FLAG::HisMX6*) were solubilized for 20 min at 0 °C in 10 ml of buffer A (20 mM Tris-HCl, pH 7.4, 500 mM NaCl, 1 mM $MnCl_2$, 1 mM $MgCl_2$, and 10% (v/v) glycerol) supplemented with 1.5% (w/v) digitonin (Calbiochem). After ultracentrifugation at 100,000 × *g* for 20 min at 4 °C, the supernatant was diluted by the addition of 20 ml of buffer A to reduce the concentration of digitonin. To immunoprecipitate the OST complex containing Ost4-FLAG, the diluted supernatant was incubated with 500 μl of anti-FLAG M2 beads (Sigma-Aldrich) for 2 h at 4 °C. After washing the beads three times with 3 ml of buffer B (20 mM Tris-HCl, pH 7.4, 100 mM NaCl, 1 mM $MnCl_2$, 1 mM $MgCl_2$, and 0.2% (w/v) digitonin), the bound materials were eluted by incubation of the washed beads twice with 750 μl of buffer B supplemented with 0.2 mg/ml 3× FLAG peptide (Sigma-Aldrich) for 30 min at 4 °C.

To further purify the OST complex, the eluate (500 μl) from anti-FLAG M2 beads was loaded onto the top of a glycerol density step gradient that consisted of 1 ml each of 10, 20, 30, and 40% (v/v) glycerol in buffer B. After ultracentrifugation at 200,000 × *g* for 2 h at 4 °C, nine fractions (500 μl each) were manually taken from the top to the bottom of the glycerol density gradient. All fractions were analyzed in parallel with bovine serum albumin as an external standard for the quantitation of OST by SDS-PAGE, followed by silver staining. The amounts of the OST complex were estimated as those of the Wbp1 subunit. The OST complex was enriched in the third and fourth fractions from the top of the glycerol density gradient.

Large Scale Preparation of DLOs—A large scale preparation of DLOs was carried out as described previously (16) with slight modifications. Yeast haploid cells BY4741 (Open Biosystems) that were transformed with pALG7 were inoculated in 6 liters of SD medium lacking leucine and incubated for 24 h at 30 °C. The cells (30,000 A_{600} units) were harvested, washed twice with 500 ml of water, and resuspended in 150 ml of lysis buffer (10 mM Tris-HCl, pH 7.4, 50 mM potassium acetate, 200 mM sorbitol, 1 mM DTT, and 2 mM EDTA). The resuspended cells were added to an equal volume of glass beads and lysed with a bead beater by three 1-min homogenizations separated by 1-min cooling periods. After centrifugation at 1,000 × *g* for 5 min, the supernatant was recovered and further centrifuged at 6,000 × *g* for 5 min. The resultant supernatant was ultracentrifuged at 100,000 × *g* for 30 min, and the microsomal pellet was resuspended in 10 ml of 20 mM Tris-HCl, pH 7.4. The microsomes were added to 50 ml of chloroform/methanol (3:2, v/v), and the mixture was vigorously agitated. After centrifugation at 2,000 × *g* for 5 min, the upper and lower liquid phases were discarded so as not to disturb the wafer at the interface between the two liquid phases. The wafer was extracted three times with 30 ml of chloroform/methanol (2:1, v/v) containing 4 mM $MgCl_2$. After centrifugation under the same conditions as described above, the pellet was dried with nitrogen gas and further extracted three times with 30 ml of methanol/water (1:1) containing 4 mM $MgCl_2$. After the centrifugation, the pellet was extracted twice with 10 ml of chloroform/methanol/water (10:10:3, v/v/v). After the centrifugation, the supernatant that contains DLOs was dried with a rotary evaporator and dissolved in 8 ml of chloroform/methanol/water (10:10:3, v/v/v). To quantitate $Glc_3Man_9GlcNAc_2$-PP-Dol (G3M9-DLO) by size fractionation HPLC, the oligosaccharide moiety was released from DLOs by mild acid hydrolysis, desalted, and labeled with 2-aminopyridine as described under "Preparation of DLOs" and "Pyridylamination."

fOS Generation Assay—The purified OST complex (1.5 pmol) was incubated for 24 h at 30 °C in 100 μl of reaction buffer (20 mM Tris-HCl, pH 7.4, 5 mM $MnCl_2$, 5 mM $MgCl_2$, 0.3 μM G3M9-DLO, 0.1% (v/v) Triton X-100, and 0.25 mg/ml phosphatidylcholine) (3). For competition assays, various concentrations of N^{α}-acetyl-Asn-Tyr-Thr (Ac-NYT) or N^{α}-acetyl-Gln-Tyr-Thr (Ac-QYT) peptide (RIKEN Research Resource Center) were added to the reaction mixture. The reaction was terminated by the addition of 300 μl of ethanol, followed by incubation for 15 min at 0 °C. After centrifugation at 15,000 × *g* for 15 min, the supernatant was evaporated to dryness. The resultant pellet was dissolved in 1 ml of water and desalted on InertSep GC column. The fOS fraction was labeled with PA as described under "Pyridylamination" and analyzed by size fractionation HPLC.

RESULTS

*fOSs Are Generated in the ER Lumen of png1*Δ *ams1*Δ *Cells*—To clarify the origin and turnover mechanism of fOSs generated via the Png1-independent process, fOSs were prepared from *png1*Δ *ams1*Δ double mutant cells of *S. cerevisiae* and were analyzed by size fractionation HPLC (Fig. 1*A*, *top*). The glycans that eluted as *peaks a–c* in Fig. 1*A* (*top*) were suscepti-

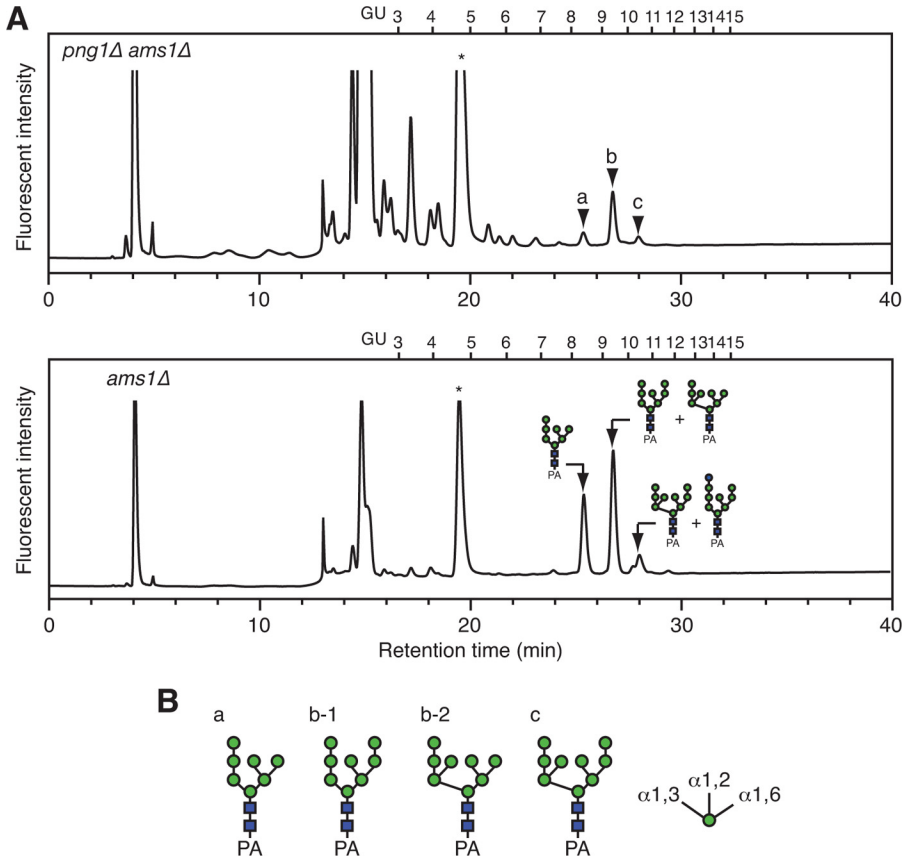

FIGURE 1. **Characterization of fOSs in yeast mutant cells.** *A*, comparison of size fractionation HPLC profiles of the PA-fOSs from *png1*Δ *ams1*Δ cells (25 A_{600} units; *top*) and *ams1*Δ cells (2.5 A_{600} units; *bottom*). The endoglycosidase H-sensitive *peaks a–c* in *png1*Δ *ams1*Δ cells are indicated by *arrowheads*. The major structures of fOSs in *ams1*Δ cells are indicated in the HPLC chart. PA-glucose oligomers (degree of polymerization = 3–15) were used as a reference, and the glucose units (*GU*) are indicated on the HPLC chart. An *asterisk* indicates the nonspecific peak derived from the labeling reagents. *B*, the major glycan structures of the PA-fOSs found in peaks *a–c* in *A*. The glycan structures were determined by their elution positions in dual-gradient, reversed-phase HPLC (14) and various α-mannosidase digestions (Table 4). Orientations of the α-mannosidic linkages are indicated on the *right*.

ble to endoglycosidase H treatment (data not shown), suggesting the presence of high mannose type glycans. Consistent with a previous report (9, 10), the amount of fOSs in *png1*Δ *ams1*Δ cells was ~4% of that in *ams1*Δ cells (Fig. 1*A* and Table 4). The main structures of fOSs generated in *png1*Δ *ams1*Δ cells were determined by dual-gradient, reversed-phase HPLC (14) and various glycosidase digestions and were found to consist of $Man_{7-9}GlcNAc_2$ (Fig. 1*B* (for the results of quantification, see Table 4)).

We next determined if these glycan isoforms were formed as a result of the action of ER glycosidases (Fig. 2*A*), particularly α-glucosidases (Gls1 and Gls2) and α-mannosidases (Mns1 and Htm1) (17). To this end, fOSs were prepared from a quintuple deletion mutant, *png1*Δ *ams1*Δ *gls1*Δ *mns1*Δ *htm1*Δ, of *S. cerevisiae*. $Glc_3Man_9GlcNAc_2$ oligosaccharide was identified as the major fOS (*peak a* in Fig. 2, *B* and *C*), suggesting that in *png1*Δ *ams1*Δ cells, the fOSs are first generated as $Glc_3Man_9GlcNAc_2$, which is then processed by glycosidases in the ER. $Glc_3Man_8GlcNAc_2$ oligosaccharide was also detected as a minor peak (*peak b* in Fig. 2, *B* and *C*). When the DLO fraction was extracted from *png1*Δ *ams1*Δ *gls1*Δ *mns1*Δ *htm1*Δ cells and analyzed by dual-gradient, reversed-phase HPLC, the identical structure was also observed (Fig. 2*D*). Because the ratio of $Glc_3Man_9GlcNAc_2$ and $Glc_3Man_8GlcNAc_2$ was similar between the fOS and DLO fractions, the truncated oligosaccharide was probably derived from the truncated DLO rather than processing by an unknown α-mannosidase in the ER glycosidase-deficient cells. We also noted that the glycans corresponding to *peaks b-2* and *c* in Fig. 1*B* were modified by the Golgi α1,6-mannosyltransferase Och1 (18, 19). Consistent with this result, a minor peak corresponding to $Glc_3Man_{10}GlcNAc_2$ was detected in the fOS fraction obtained from *png1*Δ *ams1*Δ *gls1*Δ *mns1*Δ *htm1*Δ cells (*peak c* in Fig. 2*B*).

Subcellular fractionation experiments using *png1*Δ *ams1*Δ cells revealed that over 60% of fOSs were found in the P15 fraction (Fig. 2*E*), which contains ER proteins, as judged by the enrichment of the ER chaperone Kar2 (Fig. 2*F*). This result supported our idea that fOSs produced in *png1*Δ *ams1*Δ cells are generated in the ER lumen.

fOSs Generated in the ER Lumen Are Transported to the Cytosol and Degraded by Ams1—We next examined how fOSs generated in *png1*Δ *ams1*Δ cells are catabolized. Because fOSs were not detected in the culture medium of *png1*Δ *ams1*Δ cells (data not shown), we hypothesized that they are catabolized intracellularly. To determine if Ams1 is involved in their catabolism, as is the case for the glycoprotein-derived fOSs, we first compared the structures of fOSs between *png1*Δ *ams1*Δ cells and *png1*Δ cells. As shown in Table 5, the demannosylation of fOSs occurred in *png1*Δ cells, as judged by an accumulation of

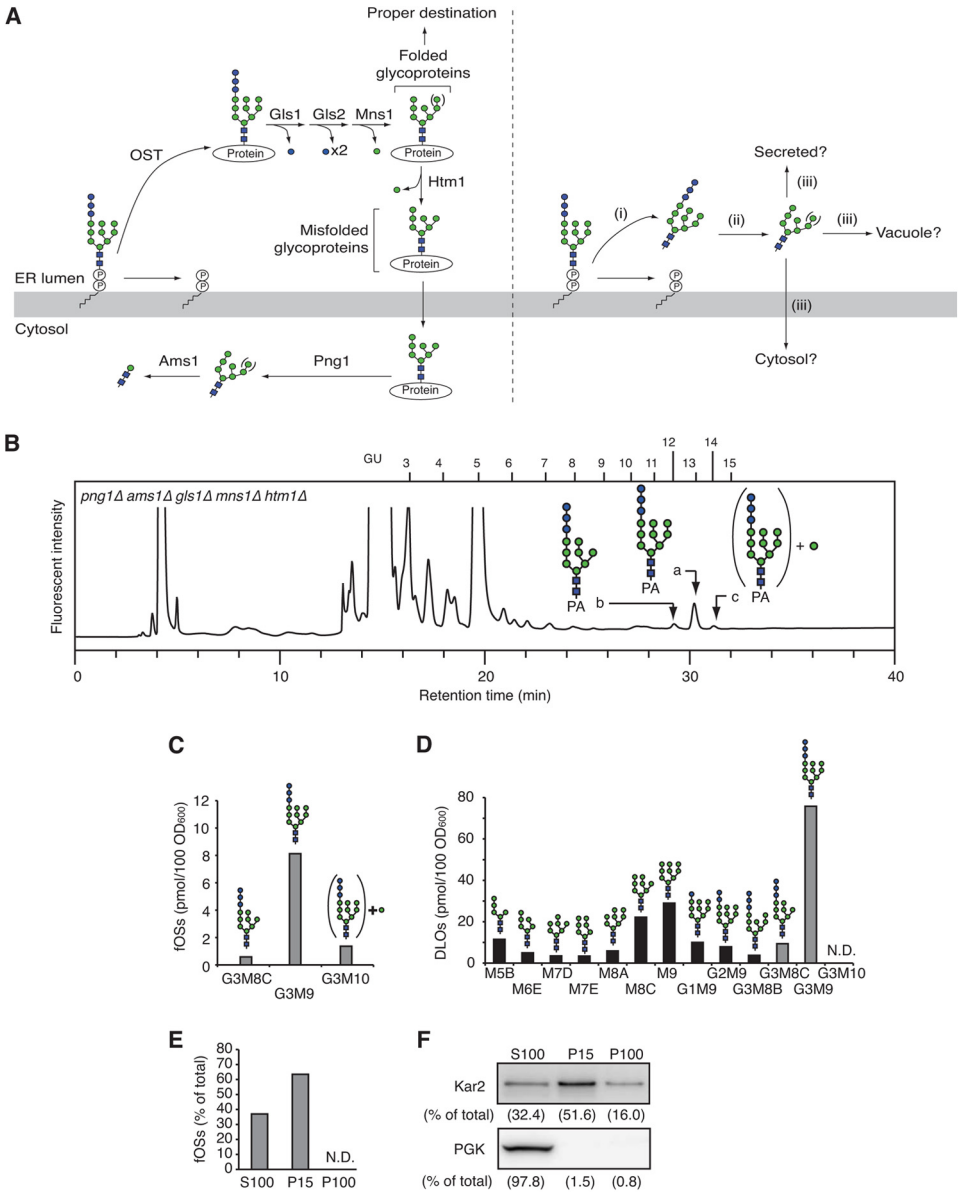

FIGURE 2. **fOSs are generated in the ER lumen and processed by the ER glycosidases.** *A*, models for the generation of fOSs by the Png1-dependent (*left*) and independent (*right*) pathways. OST transfers the oligosaccharide from $Glc_3Man_9GlcNAc_2$-PP-Dol to proteins in the ER lumen (*left*). The *N*-glycans are sequentially processed by the ER glucosidase I (*Gls1*), glucosidase II (*Gls2*), and mannosidase I (*Mns1*). If the glycoproteins are properly folded, they are destined for the target organelle. When misfolded, the glycoproteins are further processed by another ER mannosidase, Htm1. The misfolded glycoproteins are retrotranslocated to the cytosol, where Png1 releases the glycans. In the cytosol, the glycoprotein-derived fOSs are catabolized by Ams1. In the *right panel*, it is totally unknown whether fOSs are generated independently from the action of Png1 in the ER lumen in *S. cerevisiae* (*i*); whether the fOSs, if any, are processed by the ER glycosidases (*ii*); and whether they are transported and catabolized (*iii*). *B*, a size fractionation HPLC profile of fOSs from *png1*Δ *ams1*Δ *gls1*Δ *mns1*Δ *htm1*Δ cells. The major glycan structures in *peaks a–c* are indicated on the HPLC chart. PA-glucose oligomers were used as a reference, and the glucose units (*GU*) are indicated on the HPLC chart. *C*, quantitation of fOSs in *png1*Δ *ams1*Δ *gls1*Δ *mns1*Δ *htm1*Δ cells. *D*, quantitation of DLOs in *png1*Δ *ams1*Δ *gls1*Δ *mns1*Δ *htm1*Δ cells. Structural determination and quantitation of fOSs and DLOs were carried out by dual-gradient, reversed-phase HPLC (14). Note that several unusual DLO intermediates (M7D, M8A, G3M8B, and G3M8C) were generated as minor biosynthetic products in the ER glycosidase-deficient cells. *E*, subcellular fractionation experiments using *png1*Δ *ams1*Δ cells. The cells were fractionated into S100, P15, and P100 fractions by differential centrifugation. Total fOSs were set to 100%. *N.D.*, not detected. *F*, Western blot analysis of the S100, P15, and P100 fractions. *Top*, anti-Kar2 antibody; *bottom*, anti-3-phosphoglycerate kinase antibody. Percentages of the recovery of each protein are indicated in *parentheses*.

$Man_{1-6}GlcNAc_2$, indicating that Ams1 is involved in the catabolism of fOSs.

Ams1 is an α-mannosidase synthesized in the cytosol and transported to the vacuole via the cytoplasm-to-vacuole targeting pathway (20). We next addressed the question of which cellular compartment is the site for the catabolism of fOSs generated in the ER lumen. We analyzed the structures of fOSs in *png1*Δ *atg19*Δ cells. Atg19 is involved in the cytoplasm-to-vacuole targeting pathway, and in yeast cells lacking *ATG19*, Ams1 accumulates in the cytosol (20). Interestingly, when fOSs from *png1*Δ *atg19*Δ cells and *png1*Δ cells were compared, we found accumulation of $Man_{1-7}GlcNAc_2$ in *png1*Δ *atg19*Δ cells (Table 5). This result indicated that fOSs generated in the ER lumen are transported to the cytosol and efficiently degraded by the cytoplasmic Ams1. It is of note that a similar transport mechanism has been found in mammalian cells, which is mediated by

a putative oligosaccharide transporter in the ER membrane (21, 22). It should also be noted that the total amounts of fOSs are greatly increased in *png1*Δ *atg19*Δ cells by unknown mechanisms. Further studies will be needed to clarify this issue.

*OST Is Involved in the Generation of fOSs in png1*Δ *ams1*Δ *Cells*—In mammals, the fully assembled DLO substrate is thought to be hydrolyzed by unidentified mechanisms that lead to the release of the $Glc_3Man_9GlcNAc_2$ oligosaccharide (23). Previous biochemical analyses on the hydrolytic activity of calf thyroid microsomes or tissue slices (24) have suggested that OST may hydrolyze DLOs. However, no direct experimental evidence for the involvement of OST has been presented. To test whether OST is involved in the generation of fOSs in *S. cerevisiae*, the *N*-glycosylation activity of OST was impaired by gene disruptions in *png1*Δ *ams1*Δ cells. In *S. cerevisiae*, OST is a multimembrane protein complex composed of five essential gene products (Stt3p, Wbp1p, Swp1p, Ost1p, and Ost2p) and three non-essential gene products (Ost4p, Ost5p, and either Ost3p or Ost6p), which are required for optimal glycosylation activity (1). For example, a deletion of *OST5* is known to cause the mild *N*-glycosylation defects (25). Here, *png1*Δ *ams1*Δ *ost5*Δ cells showed a very weak hypoglycosylation of CPY, as visualized by the numerous bands of CPY signals in the Western blot analysis (Fig. 3*A*). Notably, the level of fOSs was also reduced by approximately half in the *OST5* deletion strain (Fig. 3*B*). A deletion of the *OST3* resulted in a more severe hypoglycosylation of CPY (Fig. 3*A*) and in a marked reduction of fOSs (Fig. 3*B*). Taken together, these data suggested that OST is involved in the generation of fOSs. In addition, we noticed that deletion of *OST6*, a paralog of *OST3*, had less effect on both *N*-glycosylation and the generation of fOSs (Fig. 3, *A* and *B*). Because it has been estimated that the Ost3-containing OST complex consists of ~80% of the total OST in *S. cerevisiae* (26), the effects of *OST6* overexpression in *png1*Δ *ams1*Δ *ost3*Δ cells on the generation of fOSs were examined. Interestingly, we found that *OST6* overexpression partially rescued the hypoglycosylation of CPY (Fig. 3*C*), whereas the level of fOSs was only slightly increased (Fig. 3*D*). By comparing the average number of *N*-glycans on CPY (Fig. 3, *A* and *C*) and the amount of fOSs (Fig. 3, *B* and *D*), it was revealed that a positive correlation exists between the glycosylation efficiency and fOS level and that the efficient generation of fOSs required a high glycosylation efficiency (>3.44 *N*-glycans/CPY molecule).

The Fully Assembled DLO Substrate Is Required for the Efficient Generation of fOSs by OST—In *S. cerevisiae*, OST has a preferred glycan specificity toward the completely assembled $Glc_3Man_9GlcNAc_2$-PP-Dol, whereas the incompletely assembled DLOs are suboptimal donor substrates for *N*-glycosylation (27). Consistent with the previous reports, a deletion of *ALG6*, which leads to the generation of DLO lacking three glucose residues, resulted in the hypoglycosylation of CPY (Fig. 3*A*) (28). Interestingly, the amount of fOSs was markedly reduced in *png1*Δ *ams1*Δ *alg6*Δ cells (Fig. 3*B*), consistent with the *in vivo* OST activity. Taken together, these data showed that OST is involved in the generation of fOSs in *S. cerevisiae* lacking Png1.

The Purified OST Complex Generates fOSs Directly from DLOs—Although we showed that the *N*-glycosylation activity of OST is important for the generation of fOSs, it was unclear

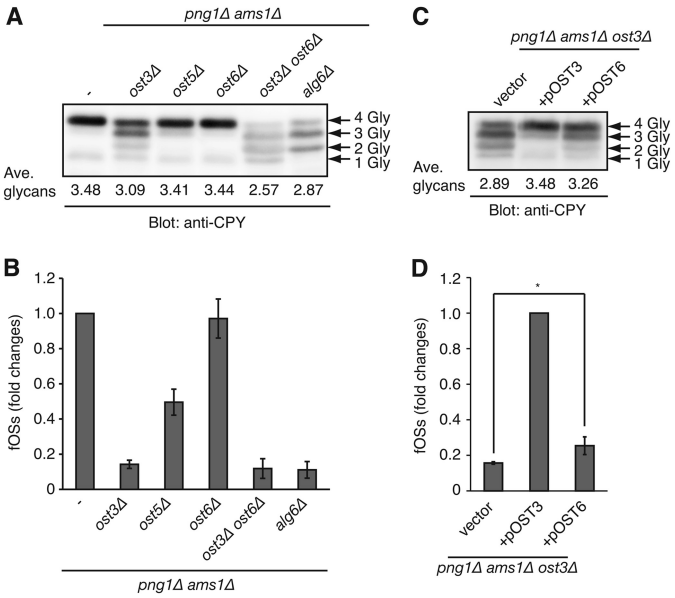

FIGURE 3. **OST is involved in the generation of fOSs.** *A*, *N*-glycosylation status of carboxypeptidase Y (CPY) in *png1*Δ *ams1*Δ cells and those lacking *OST3*, *OST5*, *OST6*, both *OST3* and *OST6*, or *ALG6*. Whole cell lysate was analyzed by Western blot with anti-CPY antibody. The number of *N*-glycans (Gly) on CPY is indicated by *arrows*. The average number of *N*-glycans on CPY was calculated by quantification of each CPY band. *B*, relative amounts of the total PA-fOSs in yeast mutant cells used in *A*. The total fOSs in *png1*Δ *ams1*Δ cells were set to 1.0. *C*, *N*-glycosylation status of CPY in *png1*Δ *ams1*Δ *ost3*Δ cells carrying empty vector (*vector*) or the plasmid encoding either *OST3* (*pOST3*) or *OST6* (*pOST6*). *D*, relative amounts of the total PA-fOSs in yeast mutant cells used in *C*. The total fOSs in *png1*Δ *ams1*Δ cells carrying pOST3 were set to 1.0. *, $p = 0.03$ (Student's *t* test). *Error bars*, S.D. from three independent experiments.

whether fOSs are directly released from DLOs because the release of fOSs can occur as a post-transfer reaction by an unclarified enzyme from glycoproteins. To address this issue, we performed an *in vitro* fOS generation assay using the immunopurified OST complex containing the FLAG-tagged Ost4 (Fig. 4*A*) and a DLO preparation. Interestingly, the incubation of OST and DLOs resulted in the formation of $Glc_3Man_9GlcNAc_2$ oligosaccharide (Fig. 4*B*), which was observed only when both OST and DLOs were present in the reaction mixture (Fig. 4*B*). Under our experimental conditions, the reaction proceeded linearly up to 24 h (data not shown). These results clearly indicated that *in vitro*, OST can hydrolyze $Glc_3Man_9GlcNAc_2$-DLO, resulting in the generation of the fOS. Next, to clarify whether the catalytic activity of OST is required for the generation of fOSs *in vitro*, the effect of EDTA, an inhibitor for the *N*-glycosylation reaction (29), was examined. Upon the addition of EDTA, the generation of fOSs by OST was completely abolished (Fig. 4*B*), supporting our findings that the *N*-glycosylation activity of OST is highly correlated with the generation of fOSs. Furthermore, co-incubation with an acceptor NYT peptide, but not with a non-acceptor QYT peptide, also reduced the generation of $Glc_3Man_9GlcNAc_2$ oligosaccharide (Fig. 4*C*), strongly indicating that *N*-glycosylation and fOS generation reactions compete the same DLO pool. Collectively, these results indicated that OST has a hydrolytic activity to DLOs *in vitro*. The specific activity of the hydrolysis by the purified OST was calculated to be 3.5 pmol/min/mg protein.

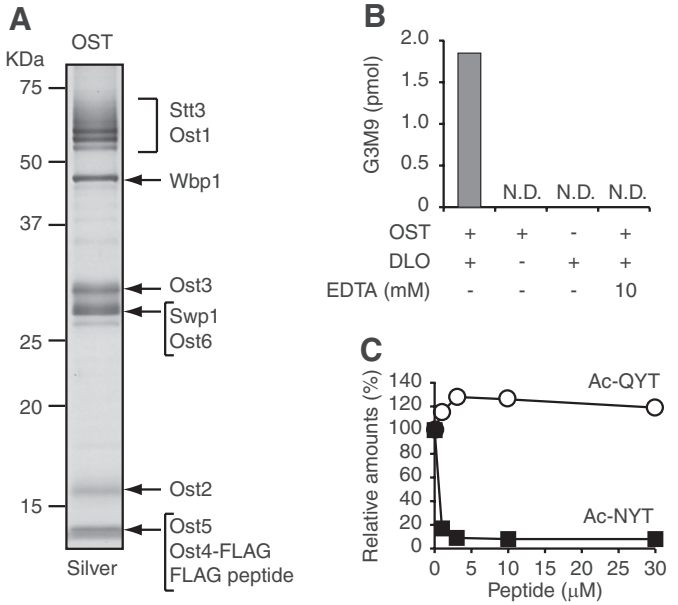

FIGURE 4. **The purified OST complex generates fOSs directly from DLOs.** *A*, SDS-PAGE of the purified OST complex (1.5 pmol), followed by silver staining. The migration positions of OST subunits were predicted based on previous reports (42, 43). *B*, *in vitro* fOS generation assay. OST, DLOs, and EDTA were incubated for 24 h in combinations as indicated at the *bottom* of the graph. After the reaction, the generated $Glc_3Man_9GlcNAc_2$ oligosaccharide (*G3M9*) was quantitated. *N.D.*, not detected. *C*, competition assay using acceptor and non-acceptor peptides. OST was incubated with DLOs in the presence or absence of various concentrations of Ac-NYT and Ac-QYT for 24 h. The amounts of G3M9 generated in the absence of the peptide were set to 100%. *Closed squares*, Ac-NYT; *open circles*, Ac-QYT.

Stt3, the Catalytic Subunit of OST, Functions in the Generation of fOSs in png1Δ ams1Δ Cells—To study the role of OST in the generation of fOSs in more detail *in vivo*, we performed analyses with a single-subunit form of OST found in kinetoplastids. The catalytic subunit of OST, Stt3, is evolutionarily conserved in all domains of life (30–32). The protozoan *Leishmania major* encodes four *STT3* paralogs (*STT3A–D*) but does not encode any other OST subunits (33–35). The expression of LmStt3D alone in *S. cerevisiae* that lacks the essential OST genes is sufficient for *N*-glycosylation activity (31, 36). We found that the expression of LmStt3D in *png1*Δ *ams1*Δ cells increases the level of fOSs (Fig. 5*A*), albeit in the presence of the fully active, endogenous OST complex. This finding demonstrated that the Stt3 protein from *L. major* mediates the generation of fOSs. Interestingly, overexpression of *S. cerevisiae* Stt3 (ScStt3) in *png1*Δ *ams1*Δ cells, but not in *png1*Δ *ams1*Δ *alg6*Δ cells, also resulted in an increase in fOSs (Fig. 5*B*). Compared with *S. cerevisiae* OST, LmStt3 has a relaxed-glycan specificity to DLOs and can efficiently utilize the incompletely assembled, non-glucosylated substrates, such as $Man_9GlcNAc_2$-PP-Dol, for *N*-glycosylation (31, 34, 36), probably due to the fact that their natural glycan donor substrate is $Man_7GlcNAc_2$-PP-Dol (34). Accordingly, a hypoglycosylation of CPY in *png1*Δ *ams1*Δ *alg6*Δ cells was partially suppressed upon the overexpression of LmStt3D (Fig. 5*C*). Notably, LmStt3D also generated fOSs efficiently in this mutant strain (Fig. 5*D*), further supporting the hypothesis that LmStt3D utilizes $Man_9GlcNAc_2$ glycans for both *N*-glycosylation and the generation of fOS.

To evaluate the functional relationship between the *N*-glycosylation and glycan-releasing activity of OST, various mutants of LmStt3D were expressed in *png1*Δ *ams1*Δ *alg6*Δ cells. In Stt3 proteins, three evolutionarily conserved motifs (D*X*D-like, WWD, and D*XX*K) have been implicated in *N*-glycosylation (30–32). Mutations of these motifs in LmStt3D resulted in a failure to improve the hypoglycosylation of CPY in *png1*Δ *ams1*Δ *alg6*Δ cells (Fig. 5*C*). As a control, it was confirmed that all of the tested LmStt3D mutations could not rescue the lethal phenotype of yeast cells lacking *STT3* (Fig. 5*E*), indicating that these motifs are critical for the function of OST. Importantly, the mutations that altered the *N*-glycosylation activity of LmStt3D also reduced the generation of fOSs (Fig. 5*F*), further supporting the idea that the *N*-glycosylation activity and fOS generation by OST are tightly linked.

The Generation of fOSs by OST Is Not Enhanced by Overproduction of the DLO Substrates—To ensure the efficient *N*-glycosylation, cells produce excess DLO substrates. One of the potential roles for the generation of fOSs is to fine tune the levels of DLO substrates by the hydrolysis. To test whether the generation of fOSs in *png1*Δ *ams1*Δ cells is regulated by the biosynthetic flux of DLO substrates, we examined the effect of an overproduction of DLO substrates. To this end, Alg7, the enzyme initiating the DLO biosynthesis, was overexpressed in *png1*Δ *ams1*Δ cells, resulting in an ~5-fold increase in the amounts of $Glc_3Man_9GlcNAc_2$-PP-Dol (Fig. 6*A*). In response to the overproduction of the DLO substrates, however, *N*-glycans and fOSs were increased only 1.4-fold (Fig. 6*B*) and 1.8-fold, respectively (Fig. 6*C*). This result indicated that overproduction of the fully assembled DLO does not result in a proportional increase of *N*-glycans and fOSs. These data suggested that, as with the case for *N*-glycosylation, the generation of fOSs by OST is not a stochastic process but is rather a highly regulated reaction.

DISCUSSION

In the present study, we provided conclusive evidence that eukaryotic OSTs generate fOSs as a consequence of the hydrolysis of DLOs in the ER lumen. Among OST subunits, we identified the catalytic Stt3 subunit as the enzyme responsible for the generation of fOSs. It has been shown that in the food-borne bacterial pathogen *Campylobacter jejuni*, the Stt3 ortholog, PglB, is responsible for the generation of fOSs (37). Periplasmic fOSs are thought to be important for the modulation of osmolarity, whereas the functional importance of fOSs in the ER remains unclear. Irrespective of function, however, our results suggested that the OST-mediated generation of fOSs may be a general feature of Stt3 proteins throughout evolution.

Comparison of specific activity between hydrolysis (3.5 pmol/min/mg protein) and *N*-glycosylation (300 pmol/min/mg protein) (3) for the purified OST complex showed that the efficiency of the hydrolytic reaction is ~1/100 that of the *N*-glycosylation reaction, indicating that the hydrolysis efficiency of OST is markedly lower than that for the *N*-glycosylation of nascent polypeptides. This result is in good agreement with the fact that PNGase-independent fOSs only account for ~4% of total fOSs. In mammalian cells, a UDP-[^{3}H]glucose labeling experiment revealed that the efficiency of fOS release was ~35% that of

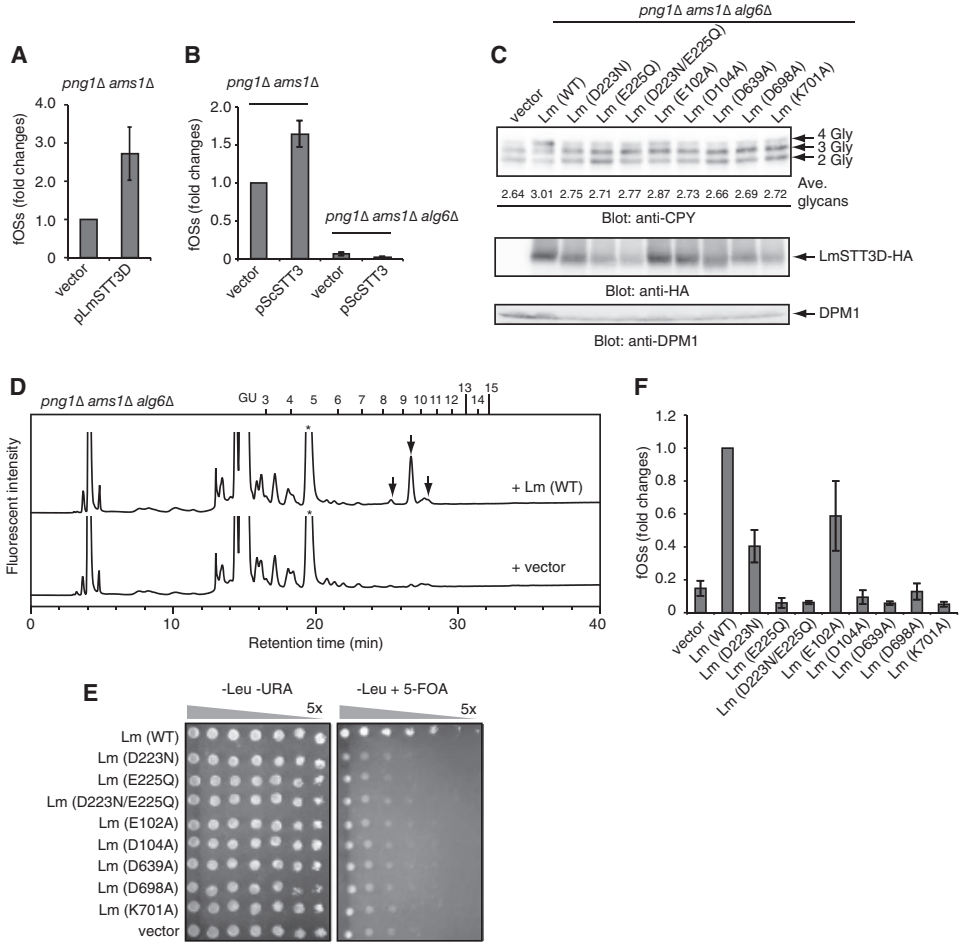

FIGURE 5. **Stt3 is responsible for the generation of fOSs.** *A*, quantitation of fOSs generated in *png1*Δ *ams1*Δ cells carrying either empty vector (*vector*) or plasmid encoding *L. major STT3D* (*pLmSTT3D*). The total fOSs from *png1*Δ *ams1*Δ cells carrying empty vector were set to 1.0. *Error bars*, S.D. from three independent experiments. *B*, quantitation of fOSs generated in *png1*Δ *ams1*Δ cells or *png1*Δ *ams1*Δ *alg6*Δ cells carrying either empty vector (*vector*) or plasmid encoding *S. cerevisiae STT3* (*pScSTT3*). The total fOSs from *png1*Δ *ams1*Δ cells carrying empty vector were set to 1.0. *Error bars*, S.D. from three independent experiments. *C*, Western blot of whole cell lysates from *png1*Δ *ams1*Δ *alg6*Δ cells carrying either empty vector (*vector*) or plasmids encoding the wild type *L. major STT3D* (*Lm* (*WT*)) and the mutants. *Top*, anti-CPY; *middle*, anti-HA (for LmStt3D-HA); *bottom*, anti-DPM1 antibodies. The number of *N*-glycans (*Gly*) on CPY is indicated on the *right*. The average number of *N*-glycans on CPY was calculated by quantification of each CPY band. *D*, size fractionation HPLC profiles of the PA-fOSs from *png1*Δ *ams1*Δ *alg6*Δ cells carrying either empty vector (*vector*) or the wild type pLmSTT3D (*Lm* (*WT*)). *Asterisks* indicate the nonspecific peak derived from the labeling reagents. *E*, plasmid shuffling assay using *stt3*Δ cells carrying the empty vector (*vector*) or the plasmid encoding LmStt3D used in *C*. 5-Fold serial dilutions of the yeast cells were spotted on the agar plate lacking leucine and uracil (*left*) and one lacking leucine supplemented with 5-fluoroorotic acid (*5-FOA*) (*right*) and then grown for 6 days at 23 °C. *F*, relative amounts of the total PA-fOSs in *png1*Δ *ams1*Δ *alg6*Δ cells carrying either the empty vector (*vector*) or the plasmid encoding the wild type (*WT*) or mutant LmStt3D. The total fOSs from *png1*Δ *ams1*Δ *alg6*Δ cells carrying pLmSTT3D (WT) were set to 1.0. *Error bars*, S.D. from three independent experiments.

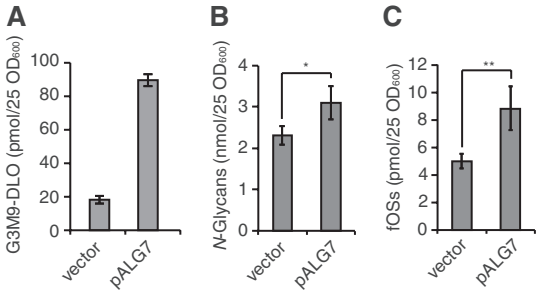

FIGURE 6. **The generation of fOSs by OST is a tightly regulated process.** Quantitation of $Glc_3Man_9GlcNAc_2$-PP-Dol (*G3M9-DLO*) (*A*), total *N*-glycans (*B*), and total fOSs (*C*) in *png1*Δ *ams1*Δ cells carrying either the empty vector (*vector*) or the plasmid encoding *ALG7* (*pALG7*). *Error bars* indicate the range of two independent experiments (*A*) and S.D. from three (*B*) or five (*C*) independent experiments. *, $p = 0.04$; **, $p = 0.001$ (Student's *t* test).

N-glycosylation after 30 min (38). The release of fOSs in mammalian cells appears to be mediated almost exclusively by PNGase-independent processes, because the knockdown of PNGase did not reduce the amount of fOSs (39). These findings imply that the efficiency of hydrolytic reaction by mammalian OST is higher than that of yeast OST.

Positive correlation between the level of fOSs and the average glycans per CPY in yeast cells lacking various OST subunits revealed a requirement of the maximum *N*-glycosylation activity of OST for the efficient generation of fOSs. This result may explain, at least in part, the reason why the overexpression of Ost6 in *png1*Δ *ams1*Δ *ost3*Δ cells barely accumulated fOSs because it resulted in an average number of glycans per CPY (3.26) below the threshold (3.41–3.44; see Fig. 3*A*) required for the efficient generation of fOSs (Fig. 3*B*). Alternatively, it is also possible that the generation of fOSs is exclusively dependent on the action of the Ost3-containing OST complex. In either case, our data clearly indicated that the presence of Ost3 or Ost6 defines the fOS generation activity of yeast OST.

Identification of fOSs modified with an additional α1,6-linked Man residue in *png1*Δ *ams1*Δ cells raised an important

question for their origin. This modification mediated by the Golgi α1,6-mannosyltransferase Och1 has been shown to occur not only on *N*-glycosylated glycoproteins destined for the cell wall compartment (18), but also on the fluorescently labeled oligosaccharides *in vitro* (40), raising the possibility that fOSs may also serve as a substrate for this glycosyltransferase. Because Och1 is localized in the Golgi (19, 41), our result may imply that a portion of fOSs may reach the Golgi and receive the modification. Alternatively, the ER-localized minor Och1 may be responsible for the modification of fOSs. In either case, because we could not detect the Och1-modified DLOs, it is unlikely that Och1 directly modifies the DLOs.

The ER-to-cytosol transport of fOSs was evident in *S. cerevisiae*. Surprisingly, an impairment of cytosol-to-vacuole transport of Ams1 promoted the demannosylation of fOSs generated in the ER, leading us to speculate that cytosolic Ams1 may have regulatory roles in the ER-to-cytosol transport of fOSs via yet unidentified mechanisms. Notably, similar ER-to-cytosol transport of fOSs has been identified in mammals, and this process has been shown to require ATP in streptolysin O-permeabilized cultured cells (21) or both ATP and the cytosol fraction in reconstituted mouse liver microsomes (22). Identification of the gene encoding the fOS transporter on the ER membrane will clarify the mechanism for the transport of fOSs as well as the function of Ams1 in this process.

We presented evidence that the reaction to generate fOSs is not regulated by the DLO pool. Interestingly, however, our *in vitro* fOS generation assay revealed that the OST complex has an ability to release fOSs directly from DLOs, implying that the binding of OST to acceptor peptides is not a prerequisite for the fOS generation reaction. Site-directed mutagenesis of LmStt3D revealed that substitution of an aspartate residue at position 223 of LmStt3D, which constitutes a potential D*X*D-like motif important for binding to divalent metal ions, to an Asn residue resulted in a loss of function of this enzyme to improve hypoglycosylation of CPY in *png1*Δ *ams1*Δ *alg6*Δ cells, but the amounts of fOSs were reduced only partially. This observation suggests that the Asp-223 residue in the D*X*D-like motif is indispensable for the *N*-glycosylation activity of OST, whereas this amino acid residue is not critical for the fOS-generation activity. Further studies, especially with an *in vitro* experiment using the purified OST enzyme, will be required to fully understand the regulatory mechanism of the OST-mediated generation of fOSs.

Irrespective of mechanism involved, the OST-mediated generation of fOSs has to be a strictly regulated reaction to ensure the efficiency and fidelity of the *N*-glycosylation. Notably, although the generation of fOSs by OST is much less active than that by Png1 in *S. cerevisiae*, the opposite situation is found in mammalian cells; PNGase-independent generation of fOSs is dominant (39). Clarification of how such regulation is achieved must await future studies.

Acknowledgments—We thank all members of the Glycometabolome Team and Dr. Shinya Hanashima (Osaka University, Japan) for fruitful discussions.

REFERENCES

1. Kelleher, D. J., and Gilmore, R. (2006) An evolving view of the eukaryotic oligosaccharyltransferase. *Glycobiology* **16,** 47R–62R
2. Helenius, A., and Aebi, M. (2004) Roles of *N*-linked glycans in the endoplasmic reticulum. *Annu. Rev. Biochem.* **73,** 1019–1049
3. Harada, Y., Li, H., Li, H., and Lennarz, W. J. (2009) Oligosaccharyltransferase directly binds to ribosome at a location near the translocon-binding site. *Proc. Natl. Acad. Sci. U.S.A.* **106,** 6945–6949
4. Ruiz-Canada, C., Kelleher, D. J., and Gilmore, R. (2009) Cotranslational and posttranslational *N*-glycosylation of polypeptides by distinct mammalian OST isoforms. *Cell* **136,** 272–283
5. Cacan, R., Hoflack, B., and Verbert, A. (1980) Fate of oligosaccharide-lipid intermediates synthesized by resting rat-spleen lymphocytes. *Eur. J. Biochem.* **106,** 473–479
6. Hanover, J. A., and Lennarz, W. J. (1981) Transmembrane assembly of membrane and secretory glycoproteins. *Arch. Biochem. Biophys.* **211,** 1–19
7. Suzuki, T., Park, H., Hollingsworth, N. M., Sternglanz, R., and Lennarz, W. J. (2000) PNG1, a yeast gene encoding a highly conserved peptide:*N*-glycanase. *J. Cell Biol.* **149,** 1039–1052
8. Suzuki, T., Seko, A., Kitajima, K., Inoue, Y., and Inoue, S. (1994) Purification and enzymatic properties of peptide:*N*-glycanase from C3H mouse-derived L-929 fibroblast cells. Possible widespread occurrence of post-translational remodification of proteins by *N*-deglycosylation. *J. Biol. Chem.* **269,** 17611–17618
9. Chantret, I., Frénoy, J. P., and Moore, S. E. (2003) Free-oligosaccharide control in the yeast *Saccharomyces cerevisiae*. Roles for peptide:*N*-glycanase (Png1p) and vacuolar mannosidase (Ams1p). *Biochem. J.* **373,** 901–908
10. Hirayama, H., Seino, J., Kitajima, T., Jigami, Y., and Suzuki, T. (2010) Free oligosaccharides to monitor glycoprotein endoplasmic reticulum-associated degradation in *Saccharomyces cerevisiae*. *J. Biol. Chem.* **285,** 12390–12404
11. Longtine, M. S., McKenzie, A., 3rd, Demarini, D. J., Shah, N. G., Wach, A., Brachat, A., Philippsen, P., and Pringle, J. R. (1998) Additional modules for versatile and economical PCR-based gene deletion and modification in *Saccharomyces cerevisiae*. *Yeast* **14,** 953–961
12. Goldstein, A. L., and McCusker, J. H. (1999) Three new dominant drug resistance cassettes for gene disruption in *Saccharomyces cerevisiae*. *Yeast* **15,** 1541–1553
13. Hase, S., Ikenaka, T., and Matsushima, Y. (1979) Analyses of oligosaccharides by tagging the reducing end with a fluorescent compound. I. Application to glycoproteins. *J Biochem.* **85,** 989–994
14. Suzuki, T., Matsuo, I., Totani, K., Funayama, S., Seino, J., Taniguchi, N., Ito, Y., and Hase, S. (2008) Dual-gradient high-performance liquid chromatography for identification of cytosolic high-mannose-type free glycans. *Anal. Biochem.* **381,** 224–232
15. Chavan, M., Chen, Z., Li, G., Schindelin, H., Lennarz, W. J., and Li, H. (2006) Dimeric organization of the yeast oligosaccharyl transferase complex. *Proc. Natl. Acad. Sci. U.S.A.* **103,** 8947–8952
16. Kelleher, D. J., Karaoglu, D., and Gilmore, R. (2001) Large-scale isolation of dolichol-linked oligosaccharides with homogeneous oligosaccharide structures. Determination of steady-state dolichol-linked oligosaccharide compositions. *Glycobiology* **11,** 321–333
17. Aebi, M., Bernasconi, R., Clerc, S., and Molinari, M. (2010) *N*-Glycan structures. Recognition and processing in the ER. *Trends Biochem. Sci.* **35,** 74–82
18. Nakayama, K., Nagasu, T., Shimma, Y., Kuromitsu, J., and Jigami, Y. (1992) OCH1 encodes a novel membrane bound mannosyltransferase. Outer chain elongation of asparagine-linked oligosaccharides. *EMBO J.* **11,** 2511–2519
19. Gaynor, E. C., te Heesen, S., Graham, T. R., Aebi, M., and Emr, S. D. (1994) Signal-mediated retrieval of a membrane protein from the Golgi to the ER in yeast. *J. Cell Biol.* **127,** 653–665
20. Shintani, T., Huang, W. P., Stromhaug, P. E., and Klionsky, D. J. (2002) Mechanism of cargo selection in the cytoplasm to vacuole targeting pathway. *Dev. Cell* **3,** 825–837

21. Moore, S. E., Bauvy, C., and Codogno, P. (1995) Endoplasmic reticulum-to-cytosol transport of free polymannose oligosaccharides in permeabilized HepG2 cells. *EMBO J.* **14,** 6034–6042
22. Haga, Y., Totani, K., Ito, Y., and Suzuki, T. (2009) Establishment of a real-time analytical method for free oligosaccharide transport from the ER to the cytosol. *Glycobiology* **19,** 987–994
23. Gao, N., Shang, J., and Lehrman, M. A. (2005) Analysis of glycosylation in CDG-Ia fibroblasts by fluorophore-assisted carbohydrate electrophoresis. Implications for extracellular glucose and intracellular mannose 6-phosphate. *J. Biol. Chem.* **280,** 17901–17909
24. Anumula, K. R., and Spiro, R. G. (1983) Release of glucose-containing polymannose oligosaccharides during glycoprotein biosynthesis. Studies with thyroid microsomal enzymes and slices. *J. Biol. Chem.* **258,** 15274–15282
25. Reiss, G., te Heesen, S., Gilmore, R., Zufferey, R., and Aebi, M. (1997) A specific screen for oligosaccharyltransferase mutations identifies the 9 kDa OST5 protein required for optimal activity *in vivo* and *in vitro*. *EMBO J.* **16,** 1164–1172
26. Spirig, U., Bodmer, D., Wacker, M., Burda, P., and Aebi, M. (2005) The 3.4-kDa Ost4 protein is required for the assembly of two distinct oligosaccharyltransferase complexes in yeast. *Glycobiology* **15,** 1396–1406
27. Lehle, L., and Bause, E. (1984) Primary structural requirements for *N*- and *O*-glycosylation of yeast mannoproteins. *Biochim. Biophys. Acta* **799,** 246–251
28. Reiss, G., te Heesen, S., Zimmerman, J., Robbins, P. W., and Aebi, M. (1996) Isolation of the ALG6 locus of *Saccharomyces cerevisiae* required for glucosylation in the *N*-linked glycosylation pathway. *Glycobiology* **6,** 493–498
29. Welply, J. K., Shenbagamurthi, P., Lennarz, W. J., and Naider, F. (1983) Substrate recognition by oligosaccharyltransferase. Studies on glycosylation of modified Asn-*X*-Thr/Ser tripeptides. *J. Biol. Chem.* **258,** 11856–11863
30. Lizak, C., Gerber, S., Numao, S., Aebi, M., and Locher, K. P. (2011) X-ray structure of a bacterial oligosaccharyltransferase. *Nature* **474,** 350–355
31. Hese, K., Otto, C., Routier, F. H., and Lehle, L. (2009) The yeast oligosaccharyltransferase complex can be replaced by STT3 from *Leishmania major*. *Glycobiology* **19,** 160–171
32. Igura, M., Maita, N., Kamishikiryo, J., Yamada, M., Obita, T., Maenaka, K., and Kohda, D. (2008) Structure-guided identification of a new catalytic motif of oligosaccharyltransferase. *EMBO J.* **27,** 234–243
33. McConville, M. J., Mullin, K. A., Ilgoutz, S. C., and Teasdale, R. D. (2002) Secretory pathway of trypanosomatid parasites. *Microbiol. Mol. Biol. Rev.* **66,** 122–154; table of contents
34. Samuelson, J., Banerjee, S., Magnelli, P., Cui, J., Kelleher, D. J., Gilmore, R., and Robbins, P. W. (2005) The diversity of dolichol-linked precursors to Asn-linked glycans likely results from secondary loss of sets of glycosyltransferases. *Proc. Natl. Acad. Sci. U.S.A.* **102,** 1548–1553
35. Ivens, A. C., Peacock, C. S., Worthey, E. A., Murphy, L., Aggarwal, G., Berriman, M., Sisk, E., Rajandream, M. A., Adlem, E., Aert, R., Anupama, A., Apostolou, Z., Attipoe, P., Bason, N., Bauser, C., Beck, A., Beverley, S. M., Bianchettin, G., Borzym, K., Bothe, G., Bruschi, C. V., Collins, M., Cadag, E., Ciarloni, L., Clayton, C., Coulson, R. M., Cronin, A., Cruz, A. K., Davies, R. M., De Gaudenzi, J., Dobson, D. E., Duesterhoeft, A., Fazelina, G., Fosker, N., Frasch, A. C., Fraser, A., Fuchs, M., Gabel, C., Goble, A., Goffeau, A., Harris, D., Hertz-Fowler, C., Hilbert, H., Horn, D., Huang, Y., Klages, S., Knights, A., Kube, M., Larke, N., Litvin, L., Lord, A., Louie, T., Marra, M., Masuy, D., Matthews, K., Michaeli, S., Mottram, J. C., Muller-Auer, S., Munden, H., Nelson, S., Norbertczak, H., Oliver, K., O'Neil, S., Pentony, M., Pohl, T. M., Price, C., Purnelle, B., Quail, M. A., Rabbinowitsch, E., Reinhardt, R., Rieger, M., Rinta, J., Robben, J., Robertson, L., Ruiz, J. C., Rutter, S., Saunders, D., Schafer, M., Schein, J., Schwartz, D. C., Seeger, K., Seyler, A., Sharp, S., Shin, H., Sivam, D., Squares, R., Squares, S., Tosato, V., Vogt, C., Volckaert, G., Wambutt, R., Warren, T., Wedler, H., Woodward, J., Zhou, S., Zimmermann, W., Smith, D. F., Blackwell, J. M., Stuart, K. D., Barrell, B., and Myler, P. J. (2005) The genome of the kinetoplastid parasite, *Leishmania major*. *Science* **309,** 436–442
36. Nasab, F. P., Schulz, B. L., Gamarro, F., Parodi, A. J., and Aebi, M. (2008) All in one. *Leishmania major* STT3 proteins substitute for the whole oligosaccharyltransferase complex in *Saccharomyces cerevisiae*. *Mol. Biol. Cell* **19,** 3758–3768
37. Nothaft, H., Liu, X., McNally, D. J., Li, J., and Szymanski, C. M. (2009) Study of free oligosaccharides derived from the bacterial *N*-glycosylation pathway. *Proc. Natl. Acad. Sci. U.S.A.* **106,** 15019–15024
38. Spiro, M. J., and Spiro, R. G. (1991) Potential regulation of *N*-glycosylation precursor through oligosaccharide-lipid hydrolase action and glucosyltransferase-glucosidase shuttle. *J. Biol. Chem.* **266,** 5311–5317
39. Chantret, I., Fasseu, M., Zaoui, K., Le Bizec, C., Yayé, H. S., Dupre, T., and Moore, S. E. (2010) Identification of roles for peptide:*N*-glycanase and endo-β-*N*-acetylglucosaminidase (Engase1p) during protein *N*-glycosylation in human HepG2 cells. *PLoS One* **5,** e11734
40. Kitajima, T., Chiba, Y., and Jigami, Y. (2006) *Saccharomyces cerevisiae* α1,6-mannosyltransferase has a catalytic potential to transfer a second mannose molecule. *FEBS J.* **273,** 5074–5085
41. Harris, S. L., and Waters, M. G. (1996) Localization of a yeast early Golgi mannosyltransferase, Och1p, involves retrograde transport. *J. Cell Biol.* **132,** 985–998
42. Karaoglu, D., Kelleher, D. J., and Gilmore, R. (1997) The highly conserved Stt3 protein is a subunit of the yeast oligosaccharyltransferase and forms a subcomplex with Ost3p and Ost4p. *J. Biol. Chem.* **272,** 32513–32520
43. Knauer, R., and Lehle, L. (1999) The oligosaccharyltransferase complex from *Saccharomyces cerevisiae*. Isolation of the OST6 gene, its synthetic interaction with OST3, and analysis of the native complex. *J. Biol. Chem.* **274,** 17249–17256
44. Kelleher, D. J., and Gilmore, R. (1994) The *Saccharomyces cerevisiae* oligosaccharyltransferase is a protein complex composed of Wbp1p, Swp1p, and four additional polypeptides. *J. Biol. Chem.* **269,** 12908–129017